

Carbohydrate-functionalized *N*-Heterocyclic Carbene Ru(II) Complexes: Synthesis, characterization and catalytic transfer hydrogenation activity

Joseph P. Byrne, Pauline Musembi, Martin Albrecht*

Department of Chemistry and Biochemistry, University of Bern, Freiestrasse 3, 3012 Bern,
Switzerland

* E-mail: martin.albrecht@dcb.unibe.ch

ABSTRACT

Three Ru complexes containing carbohydrate/*N*-heterocyclic carbene hybrid ligands were synthesized that were comprised of a triazolylidene coordination site and a directly linked peracetylated glucosyl (**5Glc**) or galactosyl unit (**5Gal**), or a glycosyl unit linked through an ethylene spacer (**6**). Electrochemical and UV-vis analysis indicate only minor perturbation of the electronic configuration of the metal center upon carbohydrate installation. Deprotection of the carbohydrate was accomplished under basic conditions to afford complexes that were stable in solution over several hours, but decomposed in the solid state. Complexes **5** and **6** were used as pre-catalysts for transfer hydrogenation of ketones under basic conditions, *i.e.* conditions that lead to *in situ* deprotection of the carbohydrate entity. The carbohydrate directly influences the catalytic activity of the metal center. Remotely linked carbohydrates (complex **6**) induce significantly lower catalytic activity than directly linked carbohydrates (complexes **5Glc**, **5Gal**), while unfunctionalized triazolylidenes are an order of magnitude more active. These observations and

substrate variations strongly suggest that substrate bonding is rate-limiting for transfer hydrogenation in these hybrid carbohydrate/triazolylidene systems.

Introduction

N-Heterocyclic carbenes (NHCs) act as versatile ligands for various catalytic systems,¹ as well as for biological and materials applications.² Ruthenium complexes of NHCs, in particular, have shown a broad range of catalytic activity,^{3–6} with application in olefin-metathesis,^{7–9} transfer hydrogenation,^{10–18} as well as oxidation of alcohols and amines,^{19–23} and water.²⁴ 1,2,3-Triazolylidenes have emerged as a particularly promising subclass of NHC ligands that are stronger σ -donors than Arduengo-type imidazolylidenes and easily accessible through Cu(I)-catalyzed azide–alkyne cycloaddition (CuAAC) ‘click’ chemistry.²⁵ Because of these characteristics, they have found widespread applications in catalysis.^{26,27} CuAAC chemistry has excellent compatibility with most functional groups due to the mild reaction conditions^{28,29} and consequently triazoles have become ubiquitous linkers for molecular components in various domains of (bio)chemistry, including materials science,^{30–32} medicinal³³ and supramolecular chemistry,^{34–37} as well as peptide/carbohydrate functionalisation.^{38–42} This CuAAC synthetic methodology allows the introduction of natural chiral pool motifs such as carbohydrates into triazoles, and thereby facilitates the decoration of 1,2,3-triazolylidene NHCs with functional wingtip substituents.^{26,43–45}

The introduction of carbohydrate substituents on the triazolylidene scaffold is particularly attractive as this approach introduces functional groups in close proximity to the metal active site. Such cooperation of ligand sites and the metal center has been demonstrated in so-called bifunctional catalysts, as introduced elegantly with Noyori-type catalysts containing an amide

functionality,^{46–48} and Shvo's catalyst featuring a proximal oxygen functionality.^{49,50} Bifunctional NHC ligands have shown promise in a range of catalytic transformations including hydrogenations, giving rise to increased catalytic activities when compared to more classical analogs.^{13,17,23,51–55}

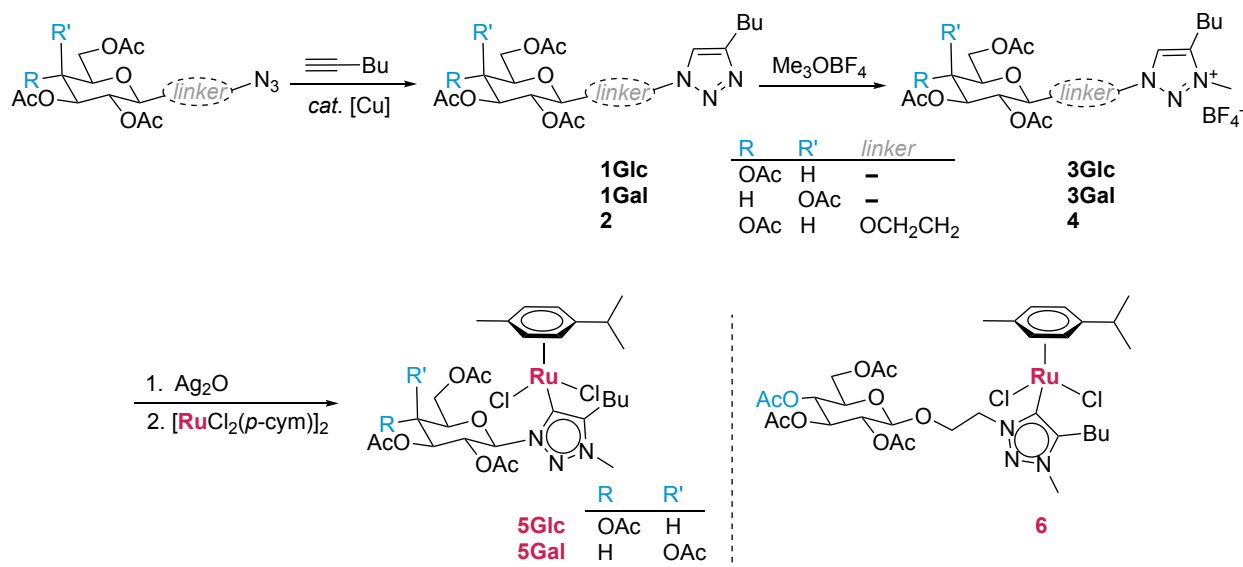
The use of carbohydrate motifs in homogenous transition metal catalysts has attracted considerable attention, particularly for introducing chirality and water solubility. Several complexes with carbohydrate-based phosphine and phosphinite ligand scaffolds have shown excellent performance in asymmetric catalysis.^{56–58} Similar work with N-heterocyclic carbene ligands, however, is much more scarce.^{59,60} In pioneering work, Dyson and co-workers investigated the anticancer activity of Ru complexes of carbohydrate-functionalized NHC ligands,^{60,61} though only few examples have explored the catalytic activity of such carbohydrate–NHC hybrid complexes.^{8,22,62} Imidazolylidene systems functionalized with two carbohydrate wingtip groups, for example, induced up to 60% *ee* in asymmetric Rh(I)-catalyzed hydrosilylation of ketones.⁶² We have demonstrated that deprotected carbohydrate substituents in NHC–Ir(III) complexes are beneficial for base-free alcohol and amine oxidation.²² Based on these results, we became interested in exploiting this ligand design motif for transfer hydrogenation.

Herein we report three novel Ru–triazolylidene complexes that incorporate carbohydrate functionality, including their photophysical and electrochemical properties as well as their catalytic activity in transfer hydrogenation of ketones, which revealed that complexes are efficiently deprotected *in situ* under the basic catalytic conditions.

Results and discussion

Synthesis and characterization

Triazole precursors **1** were synthesized in moderate yields by the CuAAC reaction from 1-hexyne and acetyl-protected anomeric azide derivatives of glucose and galactose (Scheme 1).⁶³ HRMS analysis (ESI+) confirmed formation of **1Glc** and **1Gal** by characteristic signals at $m/z = 456.1985$ and 456.1980 , respectively ($m/z = 456.1977$ calculated for $[M+H]^+$). Also, ¹H NMR analysis showed the triazolyl CH resonance for both compounds **1Glc** and **1Gal** at 7.5 ppm. Importantly, only a single anomeric proton resonance was observed for each triazole as a doublet at δ_H 5.85 and 5.81, respectively, each with a coupling constant of 9 Hz, which is consistent with stereoselective formation of β -anomers of the monosaccharide moiety. The remaining carbohydrate CH resonances differed between the glucose and galactose derivative, and the acetyl protecting groups appeared as four singlets between 1.7 and 1.3 ppm.



Scheme 1. Synthesis of complexes **5Glc**, **5Gal** and **6**.

Glycosidation of peracetylated glucopyranose with 1-bromoethanol and subsequent S_N2 reaction with NaN₃ according to literature procedures,^{64,65} yielded 1-azidoethyl-2,3,4,6-tetraacetylglucopyranoside, containing an ethylene spacer between the carbohydrate and azide functional groups. CuAAC of this azide with 1-hexyne (Scheme 1) yielded triazole **2**, which gave a signal in HRMS analysis at $m/z = 500.2236$, corresponding to [M+H]⁺ (calculated $m/z = 500.2239$). The triazolyl CH resonance appeared in the ¹H NMR spectrum at 7.21 ppm and the anomeric proton resonance was much less deshielded than in the spectra of **1**, appearing as a doublet at 4.40 ppm, which overlaps with a multiplet from the ethylene spacer. The anomeric coupling constant of 7.9 Hz is again consistent with a β-conformation.

Carbohydrate-triazole compounds **1** and **2** were alkylated with Meerwein's reagent and isolated by precipitation from methanol to afford triazolium salts **3Glc**, **3Gal** and **4** in high to quantitative yields. A diagnostic downfield shift of *ca.* 1 ppm of the triazole CH resonance was observed upon alkylation ($\delta_{\text{H}} = 8.56, 8.50$ and 8.17 , respectively) along with a new singlet corresponding to the triazolium N-methyl group. The anomeric proton resonances also shifted 0.2–0.4 ppm downfield. HRMS analysis revealed a M⁺ ion [M–BF₄]⁺ that is 14 amu higher than those of the corresponding triazole precursor [M+H]⁺ ions, indicative of successful methylation. These salts were used as ligand precursors without further purification.

Ruthenium(II) triazolylidene arene complexes **5** and **6** were synthesized from these triazolium salts via the well-established^{25,66} transmetalation procedure using Ag₂O and [RuCl₂(*p*-cym)]₂. The silver(I) carbene intermediate was not isolated, but its formation was monitored by disappearance of the triazolium CH resonance in the ¹H NMR spectrum and by HRMS analysis ($m/z = 1045.3148$ for [Ag(**3Glc**–H)₂]⁺). Isolation of the transmetalated ruthenium(II) complexes by flash chromatography provided microanalytically pure complexes **5** in good yields (60–80%), yet **6** in

a only moderate 30% yield. Successful ruthenation was confirmed by HRMS analysis, showing signals for the $[M-Cl]^+$ ion at $m/z = 740.1885$, 740.1886 and 784.2153 , for **5Glc**, **5Gal** and **6**, respectively. Complex formation was further supported via NMR analysis by the absence of the downfield 1H resonance, corresponding to a triazolium CH group in the ligand precursor, and a characteristic¹⁴ carbenic ^{13}C resonance at 167 ppm (**5**) or 163 ppm (**6**). The anomeric proton resonances in the spectra of **5** were further deshielded by 0.5–0.7 ppm when compared to the triazolium precursors and significantly broadened, appearing at δ_H 6.76 and 6.86 for **5Glc** and **5Gal**, respectively. This downfield shift indicates electronic perturbation at the anomeric position upon complexation when the carbohydrate is directly bound to the 1,2,3-triazolylidene ligand. In contrast, the shift of the anomeric resonance upon ruthenation is negligible for **6**, which contains an ethylene spacer between the triazolylidene heterocycle and the carbohydrate unit. Moreover, complex **6** features two doublet resonances in the aromatic region due to the *p*-cymene ligand in the 1H NMR spectrum, suggesting C_s symmetry of the complex. In contrast, the *p*-cymene ligand is dissymmetric in complexes **5Glc** and **5Gal** revealing four distinct resonances for the aromatic protons and two non-identical isopropyl CH_3 doublets at *ca.* 1.3 ppm for each complex. This splitting indicates restricted rotation about the $Ru-C_{NHC}$ bond and hence a more rigid second coordination sphere imparted by the directly linked carbohydrate units.

The photophysical and electrochemical properties of **5Glc**, **5Gal** and **6** in MeCN solution were probed. UV-vis absorption spectra of both the new carbohydrate-derived complexes **5** show a strong absorption band at $\lambda_{max} = 282$ nm (ϵ 5,700 $M^{-1} cm^{-1}$) as well as a shoulder at 236 nm, both tentatively attributed to ligand-centered $n-\pi^*$, $\pi-\pi^*$ transitions (Fig. 1a). In the spectrum of **6** an absorbance band at $\lambda_{max} = 272$ nm (ϵ 4,500 $M^{-1} cm^{-1}$) was observed. Additionally, all complexes

feature a broad and weak charge transfer band between 300 and 500 nm, giving rise to the yellow-orange colour of the complexes.

Electrochemical analysis using cyclic voltammetry showed two oxidations for complex **5Glc**, a quasi-reversible and presumably metal-based $\text{Ru}^{2+/3+}$ process at $E_{1/2} = +0.91$ V vs SCE and an irreversible oxidation at $E_{pa} = +1.50$ V (Fig. 1b, Table 1). **5Gal** and **6** showed very similar behavior with only slight shifts of the oxidation potentials. These redox features are reminiscent to those of the known^{14,67} ruthenium complex $[\text{RuCl}_2(\text{cym})(\text{trz}^{\text{BuBu}})]$ **7** containing two *n*-butyl wingtip groups as triazolylidene substituents ($E_{1/2} = 0.91$ V, $E_{pa} = 1.4$ V vs. SCE), indicating that the carbohydrate unit has no significant influence on the electron density at the ruthenium center, and that this unit is not redox active at these potentials.

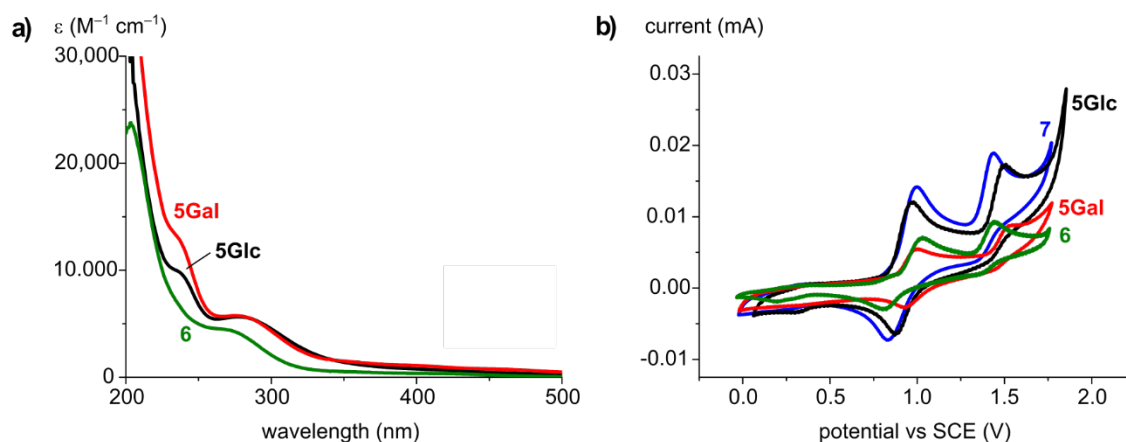


Figure 1. a) UV-Vis absorption spectra of **5Glc**, **5Gal** and **6** at room temperature in MeCN; and b) Cyclic voltammetry of **5Glc**, **5Gal**, **6**, and **7** in MeCN solution, scan rate 100 mV/s, $[\text{NBu}_4]\text{PF}_6$ as the supporting electrolyte (0.1 mM), complexes at 0.5 mM except **5Gal** (0.25 mM).

Table 1. UV-Vis spectroscopic, and electrochemical properties of complexes **5Glc**, **5Gal**, **6** and **7**^a

Complex	λ_{max} (nm) [ϵ ($\text{M}^{-1} \text{cm}^{-1}$)]	$E_{1/2}$ (V) [ΔE_p (mV)] ^b	E_{pa} (V) ^c
5Glc	282 [5,700], 236 (sh) [10,000]	0.91 [89]	1.50
5Gal	282 [5,700], 236 (sh) [13,000]	0.96 [68]	1.52

6	272 [4,500]	0.92 [226]	1.45
7	272 [4,000]	0.91 [178]	1.44

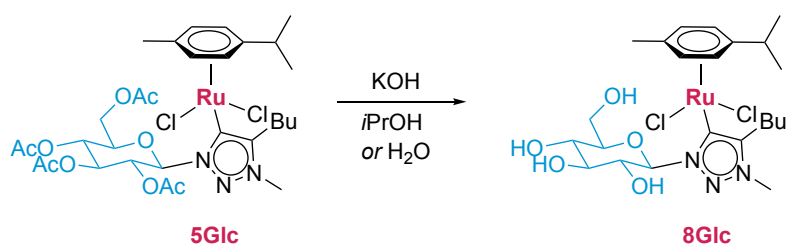
^a all measurements in MeCN, sh = shoulder; ^b all potentials vs. SCE using Fc⁺/Fc as the internal standard ($E_{1/2} = +0.40$ V, $\Delta E_p = 72$ mV), scan rate 100 mV s⁻¹, [NBu₄]PF₆ as the supporting electrolyte (0.1 mM); ^c peak potential of irreversible oxidation.

In situ deprotection of **5Glc**

Deprotection of the carbohydrate unit in complexes **5** and **6** is essential for exploiting the potential of the carbohydrate wingtip group for reductive catalytic processes and for promoting potentially bifunctional interactions involving the carbohydrate hydroxyl groups and the metal center. Such deprotection has been achieved only in a few specific cases.^{59,68,69} Recent results from our laboratory have demonstrated the deacetylation of carbohydrate wingtip groups of iridium complexes in methanolic HCl.²² The ruthenium complexes **5** and **6**, however, were not stable under these conditions and although deprotection was observed, simultaneous formation of significant amounts of free triazolium salt due to metal dissociation occurred. Acid-lability of Ru–triazolylidene bonds has been established by Grubbs, Bertrand, and co-workers in olefin metathesis catalysis.⁷ The Ru triazolylidene complexes were also not stable to conventional Zemplén deprotection conditions using methanolic NaOMe.⁷⁰ However, stability tests of complex **5Glc** under typical transfer hydrogenation conditions, *i.e.* KOH in *i*PrOH (20 mM) revealed rapid deprotection, which was accompanied by a color change of the reaction solution from orange to yellow (Scheme 2). Deprotection and formation of **8Glc** was also accomplished in D₂O using 10 equiv KOH and was confirmed by a HRMS (ESI+) signal at $m/z = 536.1684$, corresponding to [M–2Cl–H]⁺. Moreover, ¹H NMR analysis in D₂O showed the coalescence of the four distinct acetate signals of **5Glc** into a single resonance consistent with the formation of KOAc (see ESI, Figure S19). In addition, the C¹-C⁵ carbohydrate ring proton resonances are shifted upfield upon

deprotection. The asymmetry of the *p*-cymene ligand is retained, as indicated by two distinct isopropyl methyl signals at 1.13 and 1.29 ppm. Analogous results were observed for **5Gal**, suggesting wider applicability of this method.

The deprotected complex **8Glc** was not isolated as a pure solid since it displayed instability over the course of several hours upon drying. In addition, substantial amounts of degradation products were detected by ¹H NMR spectroscopy over the course of 24 h when kept in either D₂O or (CD₃)₂CDOD solution. Consequently, the more robust protected complexes **5** were used as pre-catalysts and complexes **8** were generated by *in situ* deprotection in the course of transfer hydrogenation catalysis.



Scheme 2. Synthesis of **8Glc** by base-mediated deprotection of **5Glc**.

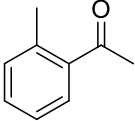
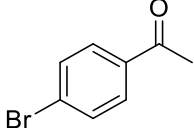
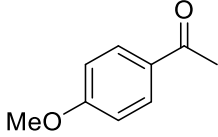
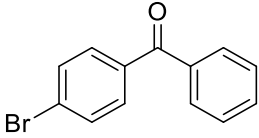
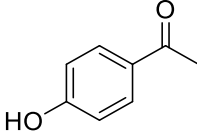
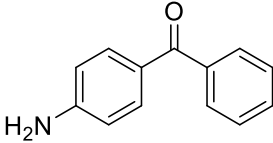
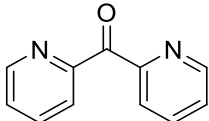
Transfer hydrogenation catalysis

To assess the suitability of the carbohydrate-functionalized carbene ruthenium complexes as pre-catalysts for base-promoted transfer hydrogenation of ketones, a model reaction with benzophenone was carried out under standard conditions,⁴³ *i.e.*, refluxing *i*PrOH as hydrogen source, KOH as activator, 100:10:1 substrate/base/complex ratio. For both **8Glc** and **8Gal**, both generated *in situ* from the acetate-protected precursors **5Glc** and **5Gal**, respectively, the reaction proceeded to completion within 8 h, forming diphenylmethanol as the exclusive product (Table 2, entries 1,2). The results for both glucose- and galactose-derivatives were essentially identical, suggesting little influence of the remote carbohydrate C4 configuration and hence no relevance of

a chair conformation of the pyranose ring⁷¹. Complex **6** featuring an ethylene spacer between the triazolylidene and carbohydrate units showed decreased activity as pre-catalyst for the model reaction, when compared to those complexes with the carbohydrate directly linked to the triazolylidene, reaching only 57% within 8 h and incomplete conversion even after 24 h (84%, entry 3). In contrast, the unfunctionalized complex **7** generates a considerably faster catalyst and reaches completion in less than 2 h ($\text{TOF}_{50} = 310 \text{ h}^{-1}$). These differences point to a direct catalytic relevance of the carbohydrate functionality, either through chelation or through stabilization of substrates or intermediates within the catalytic cycle. The location of the carbohydrate is critical and proximal oxo functionalities are less inhibiting than the more remote functional group in complex **6**.

Table 2. Catalytic activity of Ru complexes for transfer hydrogenation of various carbonyl substrates.^a

Entry	Complex	Substrate	Conversion (%) ^b		TOF ₅₀ (h ⁻¹) ^c	σ _p ^d
			8 h	24 h		
1	5Glc		98	>98	20	0
2	5Gal		>98	>98	22	0
3	6		57	84	9	0
4	7		>98	>98	310	0
5	5Glc ^e		62	>98	8	0
6	5Glc		66	98	10	0

7	5Glc		74	98	13	—
8	5Glc		56	75	8	+0.23
9	5Glc		51	77	7	-0.27
10	5Glc		62	74	11	+0.23
11	5Glc		10	16	—	-0.36
12	5Glc		15	31	—	-0.66
13	5Glc		97	>98	60	—

^a general reaction conditions: Ru complex (0.01 mmol), substrate (1.0 mmol), KOH (0.05 mL, 2 M, 0.1 mmol), 2-propanol (5 mL) at reflux; ^b determined by ¹H NMR analysis; ^c TOF₅₀ (mol product)/(mol pre-catalyst) at 50% conversion; ^d Hammett parameter of aryl *para*-substituent; ^e elemental Hg (*ca.* 1 mmol) added after 2 h.

Transfer hydrogenation of benzophenone by **5Glc** was not impeded by elemental mercury. Thus, addition of Hg (0.2 g, *ca.* 1 mmol, 100 molequiv relative to Ru) after 2 h when the reaction has reached 34% substrate conversion proceeded to full conversion (entry 5). The initial decrease of activity was attributed to mass transfer limitations induced by the mercury drop. The preservation

of catalytic activity supports a homogeneous catalyst as active species rather than significant dissociation of the triazolylidene ligand and formation of a heterogeneous layer as catalytically active phase.

Since the triazolylidene ligand is robustly coordinated to the ruthenium center, transfer hydrogenation allows for evaluating the asymmetric induction of the stereochemically well-defined carbohydrate functionality by using prochiral ketones. Similar carbohydrate-based ligands have previously been shown to be effective in asymmetric catalysis,^{58,62,72–75} including hydrosilylation of ketones.⁶² The enantioselectivity of **5Glc** was probed with acetophenone as prochiral substrate for transfer hydrogenation (entry 6). The reaction proceeded at a lower rate than with benzophenone ($\text{TOF}_{50} = 10$ vs 20 h^{-1}), reaching 66% conversion after 8 h and full conversion after 24 h. Product analysis by chiral gas chromatography revealed negligible enantioselectivity (<2%, see ESI, Figure S28), indicating that chiral information from the carbohydrate wingtip group is not transferred to the substrate under these conditions. Modification of the chiral pocket and enhanced enantioselectivity may be induced through variation of the carbohydrate, drawing on the vast pool of pyranose and ribose structures present in nature.

In order to investigate electronic and steric influences on substrate reactivity as well as functional group tolerance, a small substrate scope was carried out with derivatives of benzophenone and acetophenone using **5Glc** as pre-catalyst (entries 7–13). Using sterically more demanding 2-methylacetophenone as substrate in place of acetophenone led to a modest increase in activity ($\text{TOF}_{50} = 13$, entry 7). Very little variation of activity was noted when using electronically distinct substrates. For example, conversion of electron-withdrawing 4-bromoacetophenone ($\sigma_p = +0.23$, $\text{TOF}_{50} = 8 \text{ h}^{-1}$) and electron-donating 4-methoxyacetophenone ($\sigma_p = -0.27$, $\text{TOF}_{50} = 7 \text{ h}^{-1}$) was essentially identical (entries 8,9). Notably, neither substrate achieved full conversion after 24 h

and thus proved less suitable than unsubstituted acetophenone. 4-Bromobenzophenone showed similar activity ($\text{TOF}_{50} = 11$, entry 10), implying a markedly decreased performance with respect to the unsubstituted benzophenone. Under the same conditions, benzaldehyde was not converted to the corresponding alcohol. Alcohol and amine substituents markedly inhibited catalytic activity and ketones with these functional groups reached conversions of only 10 and 15%, respectively after 8 h (entries 11,12). In contrast, di(2-pyridyl)ketone was converted much faster than benzophenone ($\text{TOF}_{50} = 60$ vs. 20 h^{-1} , entry 13). This substrate scan suggests a few features of the catalytic transfer hydrogenation induced by **8Glc**. First, the lack of influence of electronic substituent effects on the turnover frequency indicates that the rate-limiting step is not associated with substrate conversion. Moreover, the decrease of the rate for the conversion of substituted substrates, in particular in *para* position, hints to a steric bias and the requirement of sufficient space around the metal center for turnover to proceed. This observation renders β -hydrogen elimination from coordinated isopropoxide unlikely as rate-limiting step, as this step would be substrate-independent and lead to equal rates. Instead, these data suggest instead that substrate coordination is rate-limiting, a step that is obviously affected by the steric demand and the potential (hydrogen bond) interactions of the carbohydrate with the substrate. Substrate coordination may also involve decooordination of potentially chelating carbohydrate hydroxy groups from the ruthenium center. This decooordination is accelerated with soft pyridyl coordinating groups (entry 13), which may rationalize the enhanced conversion rate observed with this substrate. In contrast, phenol and aniline functional groups are presumably too acidic and deprotonated under the basic reaction conditions, leading to a strongly coordinating ligand which is even more difficult to be displaced by the carbonyl group for catalytic turnover (entries 11,12).

Conclusions

We have successfully synthesized and characterized new carbohydrate–NHC Ru complexes. Deprotection of acetylated carbohydrate unit on the ruthenium complex was achieved *in situ* under basic conditions in protic solvents without affecting the Ru–triazolylidene bond and affording the first example of an unprotected carbohydrate–NHC system with Ru. This method provides access to hydroxy-functionalized carbene complexes, even though their isolation is compromised by stability issues. The carbohydrate functionality has a profound impact on catalytic activity in transfer hydrogenation of ketones. Directly triazolylidene-bound glucose substantially enhances turnover rates compared to more remote carbohydrate functionalization, though it reduces activity compared to unfunctionalized carbene complexes. This prominent role of the carbohydrate substituent provides opportunities for further catalyst engineering towards other transformations involving hydrogen transfer such as oxidations or hydrogen borrowing processes, as well as by modulation of the carbohydrate entity using other pyranoses or furanoses to exploit their beneficial properties in catalysis.

Experimental Section

General. Unless otherwise stated, all reagents were obtained from commercial suppliers and used as received. Carbohydrate azide precursors were prepared according to modified literature procedures.^{63–65} Ag₂O was used after regeneration by heating to >160°C under vacuum. Dry, degassed solvents were obtained by filtration over columns of dried aluminium oxide under a positive pressure of argon. NMR spectra were recorded on Bruker spectrometer operating at room temperature. Chemical shifts (δ in ppm, J in Hz) were referenced to residual solvent resonances

and are reported downfield from SiMe₄. High resolution mass spectrometry and elemental analysis were performed by the Analytical Research Services at University of Bern.

General synthesis of triazoles. Acetylated pyranosyl azide (1.000 g, 2.68 mmol) and 1-hexyne (0.31 mL, 2.7 mmol) were reacted in the presence of CuSO₄·5H₂O (0.270 g, 1.07) and sodium ascorbate (0.530 g, 2.68 mmol) in *tert*-butanol–water mixture (1:1, 20 mL), at room temperature for 3 days. The reaction mixture was diluted with EDTA (20 mL, 0.2 M in 1.0 M NH₄OH_(aq) solution) and extracted into CH₂Cl₂ (3 × 20 mL). The organic layers were combined, washed with brine, dried over MgSO₄ and filtered through Celite, yielding a white solid (**1**) or yellow oil (**2**).

1-(2,3,4,6-Tetra-O-acetyl-β-D-glucopyranosyl)-4-butyl-1,2,3-triazole (1Glc). Yield: 0.512 g, (42%). Anal. calcd. for C₂₀H₂₉N₃O₉ (455.464 g/mol): C 52.74, H 6.42, N 9.23%; found C 53.09, H 6.03, N 8.86%. HRMS (*m/z*) (ESI⁺): Calculated for C₂₀H₃₀O₉N₃⁺ [M+H]⁺ *m/z* = 456.1977; found *m/z* = 456.1985. ¹H NMR (CDCl₃, 400 MHz): δ = 0.93 (t, 3H, ³J_{H,H} = 7.5 Hz, butyl CH₃), 1.31–1.41 (m, 2H, butyl CH₂), 1.61–1.73 (m, 2H, butyl CH₂), 1.87, 2.03, 2.07, 2.08 (4 × s, 3H, C(O)CH₃), 2.72 (t, 2H, ³J_{H,H} = 7.5 Hz, C_{trz}CH₂), 3.99 (ddd, 1H, ³J_{H,H} = 9.0, 5.1, 2.1 Hz, glucosyl C⁵H), 4.14 (dd, 1H, ³J_{H,H} = 2.1 Hz, ²J_{H,H} = 12.6 Hz, glucosyl C⁶H), 4.30 (dd, 1H, ³J_{H,H} = 5.1 Hz, ²J_{H,H} = 12.6 Hz, glucosyl C⁶H), 5.23 (app t, 1H, glucosyl C⁴H), 5.34–5.49 (m, 2H, glucosyl C²H and C³H), 5.85 (d, 1H, ³J_{H,H} = 9.0 Hz, glucosyl C¹H), 7.51 (s, 1H, C_{trz}H). ¹³C {¹H} NMR (CDCl₃, 100 MHz): δ = 13.9 (butyl CH₃), 20.3, 20.66, 20.69, 20.8 (4 × C(O)CH₃), 22.3 (butyl CH₂), 25.3 (butyl CH₂), 31.3 (C_{trz}CH₂), 61.7 (glucosyl C⁶H₂), 67.9, 70.4, 72.9, 75.3 (4 × glucosyl C^{2–5}H), 85.9 (glucosyl C¹H), 119.0 (C_{trz}H), 149.5 (C_{trz}–Bu), 169.1, 169.5, 170.0, 170.6 (4 × C=O). FT-IR (ATR, cm⁻¹): 3070 (w), 2928 (w), 2357, 1746 (s, C=O), 1436, 1366, 1216 (s), 1093, 1041 (s), 928.

1-(2,3,4,6-Tetra-O-acetyl-β-D-galactopyranosyl)-4-butyl-1,2,3-triazole (1Gal). Yield: 0.560 g (46%). Anal. calcd. for C₂₀H₂₉N₃O₉ (455.464 g/mol): C 52.74, H 6.42, N 9.23%; found C 52.70, H 6.34, N 9.03%. HRMS (*m/z*) (ESI⁺): Calculated for C₂₀H₃₀O₉N₃⁺ [M+H]⁺ *m/z* = 456.1977; found *m/z* = 456.1980; calculated for C₂₀H₂₉O₉N₃Na⁺ [M+Na]⁺ *m/z* = 478.1796; found *m/z* = 478.1799. ¹H NMR (400 MHz, CDCl₃): δ = 0.94 (t, 3H, ³J_{H,H} = 7.4 Hz, butyl CH₃), 1.30–1.42 (m, 2H, butyl CH₂), 1.62–1.71 (m, 2H, butyl CH₂), 1.88, 2.01, 2.05, 2.22 (4 × s, 3H, C(O)CH₃), 2.73 (t, 2H, ³J_{H,H} = 7.4 Hz, C_{trz}CH₂), 4.11–4.24 (m, 3H, galactosyl C⁵H + C⁶H₂), 5.23 (dd, 1H, ³J_{H,H} = 10.3, 3.3 Hz, galactosyl C⁴H), 5.50–5.61 (m, 2H, galactosyl C²H + C³H), 5.81 (d, 1H, ³J_{H,H} = 9.3 Hz, galactosyl C¹H), 7.55 (s, 1H, C_{trz}H). ¹³C{¹H} NMR (100 MHz, CDCl₃): δ = 13.8 (butyl CH₃), 20.2, 20.5, 20.63, 20.64 (4 × C(O)CH₃), 22.2 (butyl CH₂), 25.3 (butyl CH₂), 31.3 (C_{trz}CH₂), 61.2 (galactosyl C⁶H₂), 66.9, 67.8, 70.9, 74.0 (galactosyl C^{2–5}H), 86.2 (galactosyl C¹H), 118.8 (C_{trz}H), 149.2 (C_{trz}-Bu), 169.1, 169.8, 169.9, 170.3 (4 × C=O); FT-IR (ATR, cm⁻¹): 2958 (w), 2929 (w), 1743 (s, C=O), 1369, 1218 (s), 1044 (s), 923.

1-(2-(4-butyl-1,2,3-triazol-1-yl)ethoxy)-1-deoxy-2,3,4,6-tetra-O-acetyl-β-D-glucopyranose (2). The product was prepared according to the general procedure from 2,3,4,6-tetra(*O*-acetyl)-1-azidoethyl-glucopyranoside (1.250 g, 2.99 mmol), yielding **2** as a pale yellow oil (1.335 g, 89%), which was used without further purification. Gradient flash chromatography (SiO₂; CH₂Cl₂ to CH₂Cl₂/CH₃OH 95:5) was used to obtain the product as an off-white hygroscopic solid. HRMS (*m/z*) (ESI⁺): Calculated for C₂₂H₃₄N₃O₁₀⁺ *m/z* = 500.2239 [M+H]⁺; found *m/z* = 500.2236. ¹H NMR (300 MHz, CDCl₃): δ = 0.92 (t, 3H, ³J_{H,H} = 7.3 Hz, butyl CH₃), 1.31–1.48 (m, 2H, butyl CH₂), 1.57–1.72 (m, 2H, butyl CH₂), 1.93, 1.98, 2.00, 2.07 (4 × s, 3H, C(O)CH₃), 2.56–2.80 (m, 2H, butyl CH₂), 3.68 (ddd, 1H, ³J_{H,H} = 10.0, 4.8, 2.4 Hz, glucosyl C⁵H), 3.90 (ddd, 1H, ²J_{H,H} = 10.4 Hz, ³J_{H,H} = 8.5, 3.4 Hz, ethylene CHH), 4.06–4.29 (m, 3H, ethylene CHH + glucosyl C⁶H₂), 4.39–

4.59 (m, 2H, ethylene CH₂), 4.46 (d, 1H, ³J_{H,H} = 7.9 Hz, glucosyl C¹H), 4.98 (dd, 1H, ³J_{H,H} = 9.5, 7.9 Hz, glucosyl C²H), 5.05 (dd, 1H, ³J_{H,H} = 10.0, 9.5 Hz, glucosyl C⁴H), 5.16 (t, 1H, ³J_{H,H} = 9.5 Hz, glucosyl C³H), 7.31 (s, 1H, C_{trz}H). ¹³C{¹H} NMR (75 MHz, CDCl₃): δ = 13.8 (butyl CH₃), 20.5, 20.5, 20.7, 20.7, (4 × C(O)CH₃), 22.3, 25.4, 31.5 (3 × butyl CH₂), 49.8 (CH₂), 61.8 (CH₂), 68.0 (CH₂), 68.3, 71.0, 72.0, 72.5 (glucosyl C²⁻⁵H), 100.6 (glucosyl C¹H), 122.0 (C_{trz}H), 148.3 (C_{trz}-Bu), 169.2, 169.4, 170.1, 170.5 (4 × C=O); FT-IR (ATR, cm⁻¹): 2935 (w), 1744 (s, C=O), 1432, 1365, 1211 (s), 1032 (s), 907.

General synthesis of triazolium salts. The triazole compound (0.44 mmol) and Me₃OBF₄ (0.067 g, 0.45 mmol) were dissolved in dry CH₂Cl₂ (30 mL) and stirred at room temperature for 16 h. Then MeOH (0.5 mL) was added and stirring continued for 30 min. All volatiles were evaporated under reduced pressure. The residue was dissolved in a minimum of MeOH and stored at -20 °C, yielding the triazolium salt as a white solid. **3Gal** and **4** were hygroscopic and were therefore used without further purification.

1-(2,3,4,6-Tetra-O-acetyl-β-D-glucopyranosyl)-4-butyl-3-methyl-1,2,3-triazol-3-ium tetrafluoroborate (3Glc). According to the general procedure, reaction of **1Glc** (0.200 g, 0.44 mmol) and Me₃OBF₄ (0.067 mg, 0.45 mmol) yielded **3Glc** (0.240 g, 98%). Anal. calcd. for C₂₁H₃₂N₃O₉BF₄ (557.303 g/mol): C 45.26, H 5.79, N 7.54%; found C 45.13, H 5.01, N 7.27%; HRMS (*m/z*) (ESI+): Calculated for C₂₁H₃₂O₉N₃⁺ [M-BF₄]⁺ *m/z* = 470.2133; found *m/z* = 470.2136. ¹H NMR (400 MHz, CDCl₃): δ = 1.00 (t, 3H, ³J_{H,H} = 7.3 Hz, butyl CH₃), 1.39–1.54 (m, 2H, butyl CH₂), 1.69–1.83 (m, 2H, butyl CH₂), 2.02, 2.03, 2.06, 2.08 (4 × s, 3H, C(O)CH₃), 2.75–2.99 (m, 2H, butyl CH₂), 4.12–4.45 (m, 6H, glucosyl C⁵H + C⁶H₂ + NCH₃), 5.26 (t, 1H, ³J_{H,H} = 9.5 Hz, glucosyl C⁴H), 5.42 (t, 1H, ³J_{H,H} = 9.5 Hz, glucosyl C³H), 5.62 (t, 1H, ³J_{H,H} = 9.0 Hz,

glucosyl C²H), 6.20 (d, 1H, ³J_{H,H} = 9.0 Hz, glucosyl C¹H), 8.56 (s, 1H, C_{trz}H). ¹³C{¹H} NMR (100 MHz, CDCl₃): δ = 13.7 (butyl CH₃), 20.5, 20.70, 20.74, 20.9 (4 × C(O)CH₃), 22.3, 23.4, 28.9 (3 × butyl CH₂), 38.4 (NCH₃), 61.2 (glucosyl C⁶H₂), 67.3, 69.6, 72.9, 75.5 (galactosyl C²⁻⁵H), 87.5 (glucosyl C¹H), 128.6 (C_{trz}H), 145.8 (C_{trz}-Bu), 169.6, 169.87, 169.93, 170.7 (4 × C=O); FT-IR (ATR, cm⁻¹): 2968 (w), 2359, 1747 (s, C=O), 1434, 1371 (s), 1215 (s), 1024 (br, s, BF₄), 927.

1-(2,3,4,6-Tetra-O-acetyl-β-D-galactopyranosyl)-4-butyl-3-methyl-1,2,3-triazol-3-ium tetrafluoroborate (3Gal). According to the general procedure, **1Gal** (0.200 g, 0.44 mmol) and Me₃OBF₄ (0.067 mg, 0.45 mmol) were reacted to yield **3Gal** (0.246 g, 100%). HRMS (*m/z*) (ESI⁺): Calculated for C₂₁H₃₂O₉N₃⁺ [M-BF₄]⁺ *m/z* = 470.2133; found *m/z* = 470.2127. ¹H NMR (300 MHz, CDCl₃): δ = 0.99 (t, 3H, ³J_{H,H} = 7.3 Hz, butyl CH₃), 1.39–1.56 (m, 2H, butyl CH₂), 1.64–1.82 (m, 2H, butyl CH₂), 2.01, 2.04, 2.07, 2.21 (4 × s, 3H, C(O)CH₃), 2.77–2.97 (m, 2H, butyl CH₂), 4.10–4.46 (m, 6H, galactosyl C⁵H + C⁶H₂ + NCH₃), 5.31 (dd, 1H, ³J_{H,H} = 10.1, 3.3 Hz, galactosyl C³H), 5.56 (d, 1H, ³J_{H,H} = 3.3 Hz, galactosyl C⁴H), 5.67 (t, 1H, ³J_{H,H} = 9.5 Hz, galactosyl C²H), 6.12 (d, 1H, ³J_{H,H} = 9.5 Hz, galactosyl C¹H), 8.50 (s, 1H, C_{trz}H). ¹³C{¹H} NMR (100 MHz, CDCl₃): δ = 13.6 (butyl CH₃), 20.4, 20.5, 20.7, 20.7 (4 × C(O)CH₃), 22.2, 23.3, 28.9 (3 × butyl CH₂), 38.2 (N-CH₃), 60.8 (galactosyl C⁶H₂), 66.8, 67.2, 70.7, 74.8 (galactosyl C²⁻⁵H), 88.0 (galactosyl C¹H), 128.0 (C_{trz}H), 145.7 (C_{trz}-Bu), 169.6, 169.9, 170.0, 170.5 (4 × C=O); FT-IR (ATR, cm⁻¹): 3121 (w), 2962 (w), 1745 (s, C=O), 1370, 1210 (s), 1034 (s, br, BF₄), 922, 496.

1-(2-(4-butyl-3-methyl-1,2,3-triazolium-1-yl)ethoxy)-1-deoxy-2,3,4,6-tetra-O-acetyl-β-D-glucopyranose tetrafluoroborate (4). According to the general procedure, **2** (0.250 g, 0.50 mmol) and Me₃OBF₄ (0.075 mg, 0.51 mmol) were reacted and yielded **4** (0.255 g, 84%). HRMS (*m/z*) (ESI⁺): Calculated for C₂₃H₃₆O₁₀N₃⁺ *m/z* = 514.2395 [M-BF₄]⁺; found *m/z* = 514.2387. ¹H NMR (400 MHz, CDCl₃): δ = 0.92 (t, 3H, ³J_{H,H} = 7.3 Hz, butyl CH₃), 1.41 (quintet, 2H ³J_{H,H} =

7.4 Hz, butyl CH₂), 1.60–1.75 (m, 2H, butyl CH₂), 1.92, 1.95, 1.96, 2.01 (4 × s, 3H, C(O)CH₃), 2.67–2.86 (m, 2H, butyl CH₂), 3.75 (ddd, 1H, *J* = 10.2, 4.7, 2.3 Hz, glucosyl C⁵H), 4.00–4.28 (m, 7H, NCH₃ + ethylene CH₂ + glucosyl C⁶H₂), 4.60 (d, 1H, ³*J*_{H,H} = 7.9 Hz, glucosyl C¹H), 4.64–4.79 (m, 2H, ethylene CH₂), 4.82 (dd, 1H, ³*J*_{H,H} = 9.6, 7.9 Hz, glucosyl C²H), 4.95 (t, 1H, ³*J*_{H,H} = 9.6 Hz, glucosyl C⁴H), 5.12 (t, 1H, ³*J*_{H,H} = 9.6 Hz, glucosyl C³H), 8.17 (s, 1H, C_{trz}H). ¹³C{¹H} NMR (100 MHz, CDCl₃): δ = 13.3 (butyl CH₃), 20.4, 20.4, 20.46, 20.53 (4 × OC(O)CH₃), 21.9, 22.7, 28.5 (3 × butyl CH₂), 37.2 (N–CH₃), 53.6 (ethylene CH₂), 61.5 (glucosyl C⁶H₂), 66.5 (ethylene CH₂), 68.1, 71.0, 71.7, 72.4 (glucosyl C^{2–5}H), 100.4 (glucosyl C¹H), 128.4 (C_{trz}H), 144.5 (C_{trz}–Bu), 169.4, 169.6, 169.8, 170.5 (4 × C=O); FT-IR (ATR, cm⁻¹): 2959 (w), 2848(w), 1744 (s, C=O), 1435, 1369, 1218 (s), 1034 (s, br, BF₄), 908.

General synthesis of Ru(II) complexes. The triazolium salt (0.43 mmol), Ag₂O (0.060 g, 0.26 mmol) and Me₄NCl (0.057 g, 0.52 mmol) were suspended in dry CH₃CN (50 mL) and stirred in the absence of light at room temperature for 5 h. The reaction mixture was diluted with CH₂Cl₂ (25 mL), filtered through Celite and concentrated under reduced pressure. CH₂Cl₂ (20 mL) and [Ru(*p*-cym)Cl₂]₂ (0.099 g, 0.16 mmol) were added and the mixture was stirred for 3 h. The reaction mixture was cooled in an ice bath, filtered through Celite, and evaporated to dryness. The red residue was purified by gradient flash chromatography (SiO₂; CH₂Cl₂ to CH₂Cl₂/Acetone 9:1).

Ru complex 5Glc. From **3Glc** (0.240 g) according to the general procedure, **5Glc** was obtained (0.189 g, 80%). Anal. calcd. for C₃₁H₄₅N₃O₉RuCl₂ (775.683 g/mol): C 48.00, H 5.85, N 5.42%; found C 48.06, H 5.39, N 5.84%. HRMS (*m/z*) (ESI⁺): Calculated for C₃₁H₄₅N₃O₉RuCl⁺ *m/z* = 740.1882 [M–Cl]⁺; found *m/z* = 740.1885. ¹H NMR (400 MHz, CDCl₃): δ = 0.95 (t, 3H, ³*J*_{H,H} = 7.3 Hz, butyl CH₃), 1.32 (d, 3H, ³*J*_{H,H} = 6.9 Hz, CHCH₃), 1.34 (d, 3H, ³*J*_{H,H} = 6.9 Hz, CHCH₃),

1.46 (quintet, 2H, $^3J_{\text{H,H}} = 7.3$ Hz, butyl CH₂), 1.54–1.64 (br s, 2H, butyl CH₂), 1.93 (s, 3H, C(O)CH₃), 1.97 (s, 3H, cym–CH₃), 2.02, 2.04, 2.06 (3 × s, 3H, C(O)CH₃), 2.88–3.08 (m, 3H, butyl CH₂ + CHMe₂), 3.97–4.09 (m, 4H, NCH₃ + glucosyl C⁵H), 4.12–4.27 (m, 2H, glucosyl C⁶H₂), 5.00 (d, 1H, $^3J_{\text{H,H}} = 5.8$ Hz, C_{cym}H), 5.14–5.26 (m, 2H, C_{cym}H + glucosyl C⁴H), 5.30–5.43 (m, 2H, C_{cym}H + glucosyl C³H), 5.53 (d, 1H, $^3J_{\text{H,H}} = 5.8$ Hz, C_{cym}H), 6.01 (t, 1H, $^3J_{\text{H,H}} = 9.4$ Hz, glucosyl C²H), 6.76 (br s, 1H, glucosyl C¹H). ¹³C{¹H} NMR (100 MHz, CDCl₃): δ = 14.0 (butyl CH₃), 18.8 (cym–CH₃), 20.71, 20.74, 20.97, 21.12 (4 × C(O)CH₃), 22.7, 23.0 (2 × CH–CH₃), 23.2 (butyl CH₂), 26.3 (butyl CH₂), 30.8 (CHMe₂), 31.8 (butyl CH₂), 37.3 (NCH₃), 62.3 (glucosyl C⁶H₂), 68.3 (glucosyl C⁴H), 70.1 (glucosyl C²H), 74.1 (glucosyl C³H), 74.5 (glucosyl C⁵H), 81.1, 81.9, 86.3, 86.8 (4 × C_{cym}H), 87.1 (glucosyl C¹H), 97.6 (C_{cym}), 108.3 (C_{cym}), 148.0 (C_{trz}–Bu), 167.1 (C_{trz}–Ru), 169.2, 169.6, 170.1, 170.5 (4 × C=O); FT-IR (ATR, cm⁻¹): 2957 (w), 1747 (s, C=O), 1433, 1365, 1212 (s), 1032, 922.

Ru complex 5Gal. From **3Gal** (0.223 g) according to the general procedure, **5Gal** was obtained (0.138 g, 60%). Anal. calcd. for C₃₁H₄₅N₃O₉RuCl₂ (775.683 g/mol), C 48.00, H 5.85, N 5.42%; found C 47.37, H 5.65, N 5.00%. HRMS (*m/z*) (ESI⁺): Calculated for C₃₁H₄₅N₃O₉RuCl⁺ *m/z* = 740.1882 [M–Cl]⁺; found *m/z* = 740.1886. ¹H NMR (400 MHz, CDCl₃): δ = 0.95 (t, 3H, $^3J_{\text{H,H}} = 7.2$ Hz, butyl CH₃), 1.30, 1.33 (2 × d, 3H, $^3J_{\text{H,H}} = 6.9$ Hz, CHCH₃), 1.40–1.55 (m, 2H, butyl CH₂), 1.60–1.90 (br s, 2H, butyl CH₂), 1.92 (s, 3H, C(O)CH₃), 1.97 (s, 3H, cym–CH₃), 1.99, 2.02, 2.23 (3 × s, 3H, C(O)CH₃), 2.85–3.14 (m, 3H, butyl CH₂ + CHMe₂), 4.08 (s, 3H, NCH₃), 4.11–4.28 (m, 3H, galactosyl C⁵H + C⁶H₂), 4.97 (d, 1H, $^3J_{\text{H,H}} = 5.8$ Hz, C_{cym}H), 5.15–5.26 (m, 2H, C_{cym}H + galactosyl CH), 5.37 (d, 1H, $^3J_{\text{H,H}} = 5.8$ Hz, C_{cym}H), 5.46–5.63 (m, 2H, C_{cym}H + galactosyl CH), 6.17 (t, 1H, $^3J_{\text{H,H}} = 9.7$ Hz, galactosyl C²H), 6.86 (br s, 1H, galactosyl C¹H). ¹³C{¹H} NMR (100 MHz, CDCl₃): δ = 14.0 (butyl CH₃), 18.8 (cym–CH₃), 20.6, 20.90, 20.92, 21.26 (4 × C(O)CH₃),

22.4 (CHCH₃), 23.2 (butyl CH₂), 26.3 (CHMe₂), 31.1 (butyl CH₂), 31.8 (butyl CH₂), 37.2 (NCH₃), 62.1 (galactosyl C⁶H₂), 67.5 (galactosyl C²H), 68.4 (galactosyl C³H), 72.1 (galactosyl C⁴H), 73.7 (galactosyl C⁵H), 80.7, 81.9, 86.0, 87.0 (4 × C_{cym}H), 87.6 (galactosyl C¹H), 98.1 (C_{cym}), 108.3 (C_{cym}), 148.0 (C_{trz}-Bu), 167.1 (C_{trz}-Ru), 169.5, 169.9, 170.27, 170.28 (4 × C=O); FT-IR (ATR, cm⁻¹): 2956 (w), 1748 (s, C=O), 1367, 1216 (s), 1051, 921.

Ru complex 6. Reaction of **4** (0.220 g) according to the general procedure afforded complex **6** (0.096 g, 30%). Anal. calcd. for C₃₃H₄₉N₃O₁₀RuCl₂·(H₂O) (837.751 g/mol), C 47.31, H 6.14, N 5.02%; found C 47.49, H 5.89, N 4.70%. HRMS (*m/z*) (ESI⁺): Calculated for C₃₃H₄₉N₃O₁₀RuCl⁺ *m/z* = 784.2144 [M-Cl]⁺; found *m/z* = 784.2153. ¹H NMR (400 MHz, CDCl₃): δ = 0.96 (t, 3H, ³J_{H,H} = 7.3 Hz, butyl CH₃), 1.30 (d, 6H, ³J_{H,H} = 6.9 Hz, CHCH₃), 1.46 (m, 2H, butyl CH₂), 1.55–1.70 (br s, 2H, butyl CH₂), 1.98 (s, 3H, C(O)CH₃), 1.99–2.04 (m, 9H, cym-CH₃ + 2 × C(O)CH₃), 2.07 (s, 3H, C(O)CH₃), 2.86–3.09 (m, 3H, butyl CH₂ + CHMe₂), 3.75 (ddd, 1H, ³J_{H,H} = 10.1, 4.6, 2.4 Hz, glucosyl C⁵H), 3.98 (s, 3H, NCH₃), 4.08–4.19 (m, 2H, ethylene CHH + glucosyl C⁶HH), 4.22–4.38 (m, 2H, ethylene CHH + glucosyl C⁶HH), 4.65 (d, 1H, ³J_{H,H} = 8.0 Hz, glucosyl C¹H), 4.83 (dtd, 2H, ²J_{H,H} = 14.0, ³J_{H,H} = 8.0, 5.8 Hz, ethylene CH₂), 4.95 (dd, 1H, ³J_{H,H} = 9.5, 8.0 Hz, glucosyl C²H), 5.07–5.14 (m, 3H, glucosyl C⁴H + C_{cym}H), 5.20 (t, 1H, ³J_{H,H} = 9.5 Hz, glucosyl C³H), 5.37 (dd, 1H, ³J_{H,H} = 5.8, 1.3 Hz, C_{cym}H), 5.40 (dd, 1H, ³J_{H,H} = 5.8, 1.3 Hz, C_{cym}H). ¹³C {¹H} NMR (100 MHz, CDCl₃): δ = 13.9 (butyl CH₃), 18.5 (cym-CH₃), 20.59, 20.61, 20.8, 22.5 (4 × C(O)CH₃), 22.8 (CHCH₃), 23.1 (butyl CH₂), 26.0 (CHMe₂), 30.7 (butyl CH₂), 31.8 (butyl CH₂), 36.4 (NCH₃), 53.8 (ethylene CH₂), 61.9 (glucosyl C⁶H₂), 68.3 (glucosyl CH), 68.7 (ethylene CH₂), 71.4, 71.9, 72.9 (3 × glucosyl CH), 82.4, 82.9, 85.1, 85.2 (4 × C_{cym}H), 96.7 (C_{cym}), 100.5 (glucosyl C¹H), 107.4 (C_{cym}), 147.6 (C_{trz}-Bu), 163.0 (C_{trz}-Ru), 169.2, 169.5, 170.1, 170.6 (4 × C=O).

In situ deprotection of 5Glc. Complex **5Glc** (4 mg, 5 μ mol) was dissolved in D₂O (0.5 mL) and KOH (0.2 M in D₂O, 0.05 mL, 0.05 mmol) was added, which induces an immediate color change from orange to yellow. HRMS (m/z) (ESI⁺): Calculated for C₂₃H₃₆N₃O₅Ru⁺ m/z = 536.1704 [M-2Cl-H]⁺; found m/z = 536.1684. ¹H NMR (300 MHz, D₂O): δ = 1.13 (d, 3H, ³J_{H,H} = 6.8 Hz, CHCH₃), 1.21 (t, 3H, ³J_{H,H} = 6.9 Hz, butyl CH₃), 1.29 (d, 3H, ³J_{H,H} = 6.8 Hz, CHCH₃), 1.61–2.10 (m, 4H, butyl CH₂), 2.08 (s, 12H, CH₃COOK) 2.24 (s, 1H, cym-CH₃), 2.52–2.72 (m, 1H, CHMe₂), 2.95–3.20 (m, 2H, butyl CH₂), 3.47–3.60 (m, 1H, glucosyl CH), 3.60–3.76 (m, 2H, glucosyl CH), 3.76–4.03 (m, 2H, glucosyl CH), 4.15 (d, 1H, J = 10.7 Hz, glucosyl C⁶H), 4.35 (s, 3H, NCH₃), 5.04–5.13 (m, 1H, C_{cym}H), 5.23 (d, 1H J = 8.2 Hz, glucosyl C¹H), 5.45 (d, 1H, ³J_{H,H} = 6.1 Hz, C_{cym}H), 5.77 (d, 1H, ³J_{H,H} = 5.7 Hz, C_{cym}H), 5.82 (d, 1H, ³J_{H,H} = 5.7 Hz, C_{cym}H).

General procedure for transfer hydrogenation catalysis. The Ru complex (0.01 mmol) was dissolved in *i*PrOH (5 mL) and aqueous KOH was added (2 M, 0.05 mL, 0.10 mmol). Hexamethylbenzene was added as an internal standard. The solution was heated to reflux for 20 min, then the ketone (1.00 mmol) was added and stirring at reflux was continued. Aliquots of the reaction mixture were sampled at given times and analyzed by diluting into CDCl₃ and measuring ¹H NMR spectra to monitor reaction progress.

Funding Sources

We acknowledge generous support from the European Commission for a Marie Skłodowska Curie Individual Fellowship to J.P.B (Grant 749549) and from the European Research Council (CoG 615653), as well as the Swiss-European Mobility Programme for a visiting fellowship for P.M. to Bern.

Supporting Information: experimental details of carbohydrate azide synthesis; ^1H and ^{13}C spectra of new compounds and HSQC spectra of deprotected complex; catalytic data; chiral gas chromatogram of acetophenone transfer hydrogenation product.

References

- 1 M. Melaimi, M. Soleilhavoup and G. Bertrand, *Angew. Chem., Int. Ed.*, 2010, **49**, 8810–8849.
- 2 L. Merce and M. Albrecht, *Chem. Soc. Rev.*, 2010, **39**, 1903.
- 3 V. Dragutan, I. Dragutan, L. Delaude and A. Demonceau, *Coord. Chem. Rev.*, 2007, **251**, 765–794.
- 4 B. Alcaide, P. Almendros and A. Luna, *Chem. Rev.*, 2009, **109**, 3817–3858.
- 5 L. Schwartsburd and M. K. Whittlesey, in *N-Heterocyclic Carbenes: Effective Tools for Organometallic Synthesis*, ed. S. P. Nolan, Wiley-VCH, 2014, pp. 341–370.
- 6 L. Delaude and A. Demonceau, in *N-Heterocyclic Carbenes: From Laboratory Curiosities to Efficient Synthetic Tools*, ed. S. Diez-Gonzalez, Royal Society of Chemistry, 2nd edn., 2017, pp. 268–301.
- 7 B. K. Keitz, J. Bouffard, G. Bertrand and R. H. Grubbs, *J. Am. Chem. Soc.*, 2011, **133**, 8498–501.
- 8 B. K. Keitz and R. H. Grubbs, *Organometallics*, 2010, **29**, 403–408.

- 9 O. M. Ogba, N. C. Warner, D. J. O’Leary and R. H. Grubbs, *Chem. Soc. Rev.*, 2018, **47**, 4510–4544.
- 10 D. A. Hey, R. M. Reich, W. Baratta and F. E. Kühn, *Coord. Chem. Rev.*, 2018, **374**, 114–132.
- 11 M. Poyatos, J. A. Mata, E. Falomir, R. H. Crabtree and E. Peris, *Organometallics*, 2003, **22**, 1110–1114.
- 12 W. Baratta, J. Schütz, E. Herdtweck, W. A. Herrmann and P. Rigo, *J. Organomet. Chem.*, 2005, **690**, 5570–5575.
- 13 R. Pretorius, Z. Mazloomi and M. Albrecht, *J. Organomet. Chem.*, 2017, **845**, 196–205.
- 14 M. Delgado-Rebollo, D. Canseco-Gonzalez, M. Hollering, H. Mueller-Bunz and M. Albrecht, *Dalton Trans.*, 2014, **43**, 4462–4473.
- 15 S. Enthaler, R. Jackstell, B. Hagemann, K. Junge, G. Erre and M. Beller, *J. Organomet. Chem.*, 2006, **691**, 4652–4659.
- 16 W. W. N. O, A. J. Lough and R. H. Morris, *Organometallics*, 2009, **28**, 6755–6761.
- 17 X.-Q. Guo, Y.-N. Wang, D. Wang, L.-H. Cai, Z.-X. Chen and X.-F. Hou, *Dalton Trans.*, 2012, **41**, 14557.
- 18 M. Hollering, M. Albrecht and F. E. Kühn, *Organometallics*, 2016, **35**, 2980–2986.
- 19 A. Prades, E. Peris and M. Albrecht, *Organometallics*, 2011, **30**, 1162–1167.
- 20 A. Bolje, S. Hohloch, D. Urankar, A. Pevec, M. Gazvoda, B. Sarkar and J. Košmrlj,

- Organometallics*, 2014, **33**, 2588–2598.
- 21 B. Bagh, A. M. McKinty, A. J. Lough and D. W. Stephan, *Dalton Trans.*, 2014, **43**, 12842–12850.
- 22 R. Pretorius, J. Olguin and M. Albrecht, *Inorg. Chem.*, 2017, **56**, 12410–12420.
- 23 S. Hohloch, L. Hettmanczyk and B. Sarkar, *Eur. J. Inorg. Chem.*, 2014, **2014**, 3164–3171.
- 24 L. Bernet, R. Lalrempuia, W. Ghattas, H. Mueller-Bunz, L. Vigara, A. Llobet and M. Albrecht, *Chem. Commun.*, 2011, **47**, 8058.
- 25 P. Mathew, A. Neels and M. Albrecht, *J. Am. Chem. Soc.*, 2008, **130**, 13534–13535.
- 26 K. F. Donnelly, A. Petronilho and M. Albrecht, *Chem. Commun.*, 2013, **49**, 1145–1159.
- 27 Á. Vivancos, C. Segarra and M. Albrecht, *Chem. Rev.*, 2018, **118**, 9493–9586.
- 28 V. V. Rostovtsev, L. G. Green, V. V. Fokin and K. B. Sharpless, *Angew. Chemie*, 2002, **114**, 2708–2711.
- 29 C. W. Tornøe, C. Christensen and M. Meldal, *J. Org. Chem.*, 2002, **67**, 3057–3064.
- 30 W. H. Binder and R. Sachsenhofer, *Macromol. Rapid Commun.*, 2007, **28**, 15–54.
- 31 J. A. Johnson, M. G. Finn, J. T. Koberstein and N. J. Turro, *Macromol. Rapid Commun.*, 2008, **29**, 1052–1072.
- 32 P. L. Golas and K. Matyjaszewski, *Chem. Soc. Rev.*, 2010, **39**, 1338–1354.
- 33 H. C. Kolb and K. B. Sharpless, *Drug Discovery Today*, 2003, **8**, 1128–1137.

- 34 J. D. Crowley and P. H. Bandeen, *Dalton Trans.*, 2010, **39**, 612–623.
- 35 J. D. Crowley, S. M. Goldup, A.-L. Lee, D. A. Leigh and R. T. McBurney, *Chem. Soc. Rev.*, 2009, **38**, 1530.
- 36 J. P. Byrne, S. Blasco, A. B. Aletti, G. Hessman and T. Gunnlaugsson, *Angew. Chem., Int. Ed.*, 2016, **55**, 8938–8943.
- 37 J. P. Byrne, J. A. Kitchen, J. E. O'Brien, R. D. Peacock and T. Gunnlaugsson, *Inorg. Chem.*, 2015, **54**, 1426–1439.
- 38 J. M. Holub and K. Kirshenbaum, *Chem. Soc. Rev.*, 2010, **39**, 1325.
- 39 X. Liu, R. B. P. Elmes and K. A. Jolliffe, *Aust. J. Chem.*, 2017, **70**, 201.
- 40 V. K. Tiwari, B. B. Mishra, K. B. Mishra, N. Mishra, A. S. Singh and X. Chen, *Chem. Rev.*, 2016, **116**, 3086–3240.
- 41 C. Bouillon, A. Meyer, S. Vidal, A. Jochum, Y. Chevolot, J. P. Cloarec, J. P. Praly, J. J. Vasseur and F. Morvan, *J. Org. Chem.*, 2006, **71**, 4700–4702.
- 42 M. Milne, K. Chicas, A. Li, R. Bartha and R. H. E. Hudson, *Org. Biomol. Chem.*, 2012, **10**, 287–292.
- 43 S. Horn, C. Gandolfi and M. Albrecht, *Eur. J. Inorg. Chem.*, 2011, **2011**, 2863–2868.
- 44 A. Monney, G. Venkatachalam and M. Albrecht, *Dalton Trans.*, 2011, **40**, 2716.
- 45 J. D. Crowley, A.-L. Lee and K. J. Kilpin, *Aust. J. Chem.*, 2011, **64**, 1118–1132.

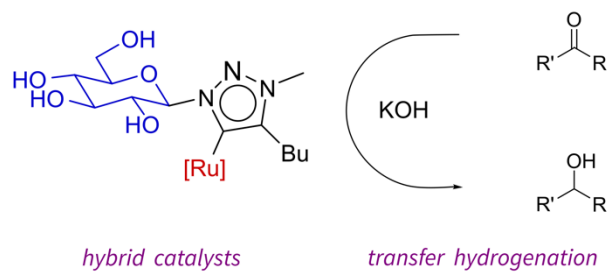
- 46 R. Noyori and S. Hashiguchi, *Acc. Chem. Res.*, 1997, **30**, 97–102.
- 47 R. Noyori, M. Yamakawa and S. Hashiguchi, *J. Org. Chem.*, 2001, **66**, 7931–7944.
- 48 T. Ohkuma, N. Utsumi, K. Tsutsumi, K. Murata, C. Sandoval and R. Noyori, *J. Am. Chem. Soc.*, 2006, **128**, 8724–8725.
- 49 Y. Shvo, D. Czarkie, Y. Rahamim and D. F. Chodosh, *J. Am. Chem. Soc.*, 1986, **108**, 7400–7402.
- 50 B. L. Conley, M. K. Pennington-Boggio, E. Boz and T. J. Williams, *Chem. Rev.*, 2010, **110**, 2294–2312.
- 51 W. W. N. O, A. J. Lough and R. H. Morris, *Chem. Commun.*, 2010, **46**, 8240.
- 52 W. B. Cross, C. G. Daly, Y. Boutadla and K. Singh, *Dalton Trans.*, 2011, **40**, 9722.
- 53 A. Bartoszewicz, R. Marcos, S. Sahoo, A. K. Inge, X. Zou and B. Martín-Matute, *Chem. - Eur. J.*, 2012, **18**, 14510–14519.
- 54 A. Bartoszewicz, G. González Miera, R. Marcos, P. O. Norrby and B. Martín-Matute, *ACS Catal.*, 2015, **5**, 3704–3716.
- 55 G. González Miera, E. Martínez-Castro and B. Martín-Matute, *Organometallics*, 2018, **37**, 636–644.
- 56 S. Woodward, M. Diéguez and O. Pàmies, *Coord. Chem. Rev.*, 2010, **254**, 2007–2030.
- 57 S. Castellón, C. Claver and Y. Díaz, *Chem. Soc. Rev.*, 2005, **34**, 702.

- 58 A. S. Henderson, J. F. Bower and M. C. Galan, *Org. Biomol. Chem.*, 2016, **14**, 4008–4017.
- 59 W. Zhao, V. Ferro and M. V. Baker, *Coord. Chem. Rev.*, 2017, **339**, 1–16.
- 60 K. J. Kilpin, S. Crot, T. Riedel, J. A. Kitchen and P. J. Dyson, *Dalton Trans.*, 2014, **43**, 1443–1448.
- 61 K. Purkait, S. Karmakar, S. Bhattacharyya, S. Chatterjee, S. K. Dey and A. Mukherjee, *Dalton Trans.*, 2015, **44**, 5969–5973.
- 62 A. S. Henderson, J. F. Bower and M. C. Galan, *Org. Biomol. Chem.*, 2014, **12**, 9180–9183.
- 63 H. Paulsen, Z. Györgydeák and M. Friedmann, *Chem. Ber.*, 1974, **107**, 1568–1578.
- 64 P. Quagliotto, G. Viscardi, C. Barolo, D. D'Angelo, E. Barni, C. Compari, E. Duce and E. Fiscaro, *J. Org. Chem.*, 2005, **70**, 9857–9866.
- 65 S. M. Paterson, J. Clark, K. A. Stubbs, T. V. Chirila and M. V. Baker, *J. Polym. Sci. Part A Polym. Chem.*, 2011, **49**, 4312–4315.
- 66 H. M. J. Wang and I. J. B. Lin, *Organometallics*, 1998, **17**, 972–975.
- 67 D. Canseco-Gonzalez and M. Albrecht, *Dalton Trans.*, 2013, **42**, 7424.
- 68 C. C. Yang, P. S. Lin, F. C. Liu, I. J. B. Lin, G. H. Lee and S. M. Peng, *Organometallics*, 2010, **29**, 5959–5971.
- 69 Y. Imanaka, H. Hashimoto, I. Kinoshita and T. Nishioka, *Chem. Lett.*, 2014, **43**, 687–689.
- 70 B. Ren, M. Wang, J. Liu, J. Ge, X. Zhang and H. Dong, *Green Chem.*, 2015, **17**, 1390–

1394.

- 71 J. J. Topczewski, P. J. Cabrera, N. I. Saper and M. S. Sanford, *Nature*, 2016, **531**, 220–224.
- 72 M. T. Reetz and T. Neugebauer, *Angew. Chem., Int. Ed.*, 1999, **38**, 179–181.
- 73 M. Guitet, P. Zhang, F. Marcelo, C. Tugny, J. Jiménez-Barbero, O. Buriez, C. Amatore, V. Mouriès-Mansuy, J. P. Goddard, L. Fensterbank, Y. Zhang, S. Roland, M. Ménand and M. Sollogoub, *Angew. Chem., Int. Ed.*, 2013, **52**, 7213–7218.
- 74 J. F. Moya, C. Rosales, I. Fernández and N. Khair, *Org. Biomol. Chem.*, 2017, **15**, 5772–5780.
- 75 M. Coll, O. Pàmies and M. Diéguez, *Adv. Synth. Catal.*, 2014, **356**, 2293–2302.

For Table of Contents Use Only



Triazolylidene NHCs were decorated with a carbohydrate wingtip group and complexed to a ruthenium(II) center. Deprotection of the carbohydrate while bound to the metal center affords a carbohydrate-NHC hybrid system which has been used as transfer hydrogenation catalyst.